ASME 2013 Summer Heat Transfer Conference, HT2013
July 14-19, 2013, Minneapolis, MN, USA

HT2013-17690

Hypersonic Liquefaction in the Cryogenic Zone

Charl E Janeke (PE) / Kartago Inc, Los Angeles CA 90017

ABSTRACT

In order to improve the payload economics and complexity of state-of-the-art orbital launch systems inclusive of the Soyuz and SpaceX Falcon, atmospheric acceleration and air-breathing rockets is a must to abate the burden and cost of tanked oxygen that constitutes +50% of the takeoff weight of existing orbital launching means. However common logic dictates that in order to rationally suffice as a launching platform, a hypersonic rocket OR aerospace plane must be capable of generating + 50% of the orbital kinetic energy (+Mach 17) by own means. Because shockwave formation is an endemic problem with speeds in excess of Mach-3, the challenge therefore has been devising means of shockwave abatement, kinetic conversion and SCRAM combustion in support of atmospheric speeds in excess of Mach 15.

The quest for hypersonic shockwave piercing and oxygen liquefaction led to the Virginia Tech Space and Ocean Laboratory through the CRYSONIX© small business entitlement program that resulted in the worlds 1st hypersonic shockwave piercing event www.crysonix.com July 2010 that culminated in the May 2013 SPINNX© (extreme) hypersonic vortex transformation tests. The quest for (extreme) hypersonic vortex transformation was the result of an independent Los Angeles developed HiRE© (hypersonic) SCRAM combustion protocol that is vortex driven. This treatise will focus on the computational dynamics of oxygen liquefaction in the cryogenic zone.

CONTENTS

1. The Algebra of Liquefaction

Transient heat conduction is controlled by the generalized Fourier 2nd order DE of heat flow;

$$\partial T/\partial t = \alpha\underline{\Delta}T + Qs/\rho Cp \quad \text{……………………………………………………(1)}$$

.

where ∂T/∂t denotes the partial time-temperature derivative, $\underline{\Delta}T$ the 2nd order spatial temperature distribution, Qs the heat production/sink per unit volume, α / ρ / Cp the thermal diffusivity / density / specific heat respectively of saturated oxygen at 250R (the case study conditions). In event of a one-dimensional flow field the generalized Fourier DE of heat flow defaults to;

$$dT/dt = \alpha dT/dx^2 + Qs'/\rho Cp \quad \text{……………………………………………………..(2)}$$

where dT/dt denotes the 1st order temperature-time derivative, dT/dx^2 the 2nd order temperature dispersion in the X-plane and Q's the unit heat production/sink in the X-plane that may be rewritten in finite notation as;

$$\Delta T/\Delta t = \alpha(\Delta T/\Delta x)/\Delta x + Qs'/\rho Cp \quad \text{………………………………………..….(3)}$$

By substituting Δt with $\Delta\Gamma = \Delta L^2/2\alpha$ (the Schmidt time-gain equivalency) and dropping the source term $Qs'/\rho Cp$, equation (3) may be rewritten as;

$\Delta T/\Delta\Gamma = \Delta T(\Delta L)/2$ or $\Delta T = \Delta\Gamma(\Delta T(\Delta L))/2$……………………………….…..(4)

By hence taking time limits n-1 to n to n+1 for a finite slab ΔL, the transient equation system (4) may be transformed into the classical Binder-Schmidt recursive differencing system;

$T(n, n+1) = [T(n+1, n)+T(n-1, n)]/2$…….(5)

subject to the Schmidt equivalency $\Delta\Gamma = \Delta L^2/2\alpha$, where $T(n, n+1)$ denotes the incremental temperature increase of a finite slab Δx through the n to (n+1) the time indexes, $[T(n+1, n) + T(n-1, n)] / 2$ the mean temperature of the finite slab ΔL through the (n+1, n) (new) and (n-1, n) (old) time indexes, Qs'' the unit heat production/sink for the finite slab ΔL and k the heat conductivity of saturated oxygen at 250R.

In accordance with the Binder-Schmidt system http://www.egi.kth.se/courses/4A1601/Files/lab3HT.pdf (p9) the transient heat conduction in a (homogeneous) solid material may be equated as the intersection of the time indexing lines (time index "n"and finite layers "m") on a drafting board that constituted a giant computational advance for mankind in the age of ratchet calculators and punch-card tabulators.

In order to devise an adaptive computational model for the freezing of molten steel as a working tool in 1965, the heat source term $Qs'/\rho Cp$ was reinstated into the native Binder-Schmidt model by equating $Qs'/\rho Cp = Qs''/k$ in accordance with the Schmidt equivalency $\Delta\Gamma = \Delta L^2/2\alpha$, that rendered the modified Binder-Schmidt (MBS) difference system;.

$T(n, n+1) = \alpha[T(n+1, n)+T(n-1, n)]/2 + \Sigma[dT(n, M)]$ …………………..……..(6)

By equating $\Sigma[dT(n, M)] = Qs''/k$ as the latent MBS transformation, latent gain function $dT(n, M)$ of the finite layer M may be equated as the sum of the incremental temperature gradients $dT(n, M) >> dT(N, M)$ in satisfaction of the change-of-phase condition $\Sigma[\Delta(TM)] = Qs''/k$ over the incremental time span $n >> N$. The real-time implication is that the computational system is "frozen" at layer M until the condition $\Sigma[dT(n, M)] = Qs''/k$ has been satisfied. The methodology was validated (1967 MS thesis) (supra) via (1) a molten wax lab model with thermocouple sensors (2) GAUS-ERROR and EULER (exact) DE solutions with step-function boundary conditions and (3) a FORTRAN computational model that morphed the MBS "source" transformation.

With the coming of age of the PC and infinite spreadsheet computing power the MBS was transformed into (million year) incremental spreadsheet computational model in July 2009 to emulate the transients of formation of the crust of the earth in pursuit of a global (greenhouse) heat load / equilibrium model www.polarequilibrium.com. In contrast to the 2009 global greenhouse model with 32M year time increments, the resulting 2013 MBS (hypersonic) liquefaction scale ranges from 1/100sec to 1/1000sec in accordance with the Schmidt equivalency $\Delta\Gamma = \Delta L^2/2\alpha$, vs. 2sec intervals for the 1965 wax model differencing platform.

2. The MBS Liquefaction Model

Since starting the hypersonic (air-breathing) aerospace plane initiative the tantalizing question was (1) how to beat shockwaves through Mach-20 (2) how to extract/distill liquid oxygen out of ambient air in the hypersonic domain and (3) how to generate enough liquid oxygen to power a rocket engine to drive the aerospace plane through the +Mach-10 domain into space. Having conjectured many schemes and ultimately running out of feasible options, inventive testing (the cryogenic copperball hyperbole) was elected as the route to unlock the liquefaction enigma. Having hit stumbling block #2 the Directorate of the Space and Ocean Laboratory at Virginia Tech considered the liquefaction quest substantive and granted small business facilitation to the hypersonic lab that spawned the Crysonix© "piercing" program June 2010. With a Pandora box of parts the 1st cryogenic test was run with a 11/8" diameter copper ball July 29, 2010 at –140C and a 2nd test at –160C July 30, 2010. Although nothing significant was observed in situ, closer analysis of the Schlieren recordings thereafter showed (1) a definitive piercing / liquefaction window in concurrence with the saturation curve of oxygen at –140 to –150C @15-20atm (2) distinctive harmonic surging and (3) powerful after the fact (superfluid) circulation/spinning. The age of the (hypersonic) liquefaction nosecone has been born. The initial small steps rapidly turned into giant leaps that lead to the SPINNX© (extreme vortex formation) synthesis three years (May 2013) later. See schematic apparatus graphics Figure 1.

Having documented the rules of (hypersonic) liquefaction, shockwave piercing and (extreme) vortex formation in the cryogenic zone succinctly, the focus turned to computational modeling. Because of the intrinsic harmonic nature of the piercing phenomenon with violent staccato pressure surges, the focus is on the liquefaction transients as the controlling (surging) denominator. Therefore the focus on the modified Binder-Schmidt (MBS) modeling system where by thermal dispersion, elemental layering and liquefaction saturation may be succinctly monitored and corrected vs. the black-box CFD input / output protocol.

In accordance with the MBS protocol the time function $\Delta\Gamma = \Delta L^2/2\alpha$ may be equated as $\Delta\Gamma$ = 3600x (0.01/12)^2/2/2.0 = **0.00062sec** for the finite layer system **ΔL = 0.01inch** given the dimensionless thermal diffusivity of the incipient (compressed) hypersonic front as $\alpha = k/\rho Cp$ = 0.22/(0.015x0.22) = **2.0**.

The MBS spreadsheet is hence constructed out of the following components;

PART 1: The incremental time module;
PART 2: Differencing module boundary conditions;
PART 3: The heat of transformations source terms;
PART 4: The structured computational model;
PART 5: The terminal saturation stage;
PART 6: The spreadsheet model.

The computational model has been based on Mach-5 liquefaction dynamics with an estimated (reheated) expansion temperature of –105C (the initial conditions), a supercool reaction plane of –160C and the liquefaction temperature of –140C at 30x atmospheres that equated to 300 / 200 / 240 on the Renkine scale respectively as per PART 4. Noteworthy is that the boundary vector k/h = 0.44/100 drives the –105C temperature of the incipient hypersonic blast down to the supercool reaction plane temperature of –160C virtually instantaneously as per Figure 2 (PART 6 graphics). The magic of supercooling may hence be simply equated to a step function in the Z plane.

The principal challenges at task however are (1) determine the rate of oxygen liquefaction and (2) determining the surging trigger threshold. Whereas liquefaction initiates at time step #2 (viz. 0.00124sec on the absolute time scale (PART 4), liquefaction stalls at time step #100 (viz. 0.062sec on the absolute time scale) (PART 5). When liquefaction ceases the boundary layer (**0.03inch** in the latter event) will collapse and spawn a new liquefaction recursion. The resulting recursions will hence generate **16.13Hz** harmonics. However because the rapid initial rate of liquefaction, liquid oxygen discharge may be triggered may be triggered at the 0.01sec threshold (PART 4) resulting **100Hz** stochastic distribution at the top end of the scale. Compare CHAOS where (1) the system does not conform to any rule and (2) the outcome is totally unpredictable. See illustrative graphics Figures 3/4.

3. LO2 Production Rate

In order to built a functional (air breathing) hypersonic aerospace plane the oxygen liquefaction capacity must be perfectly predictable and manageable. The question therefore is whether the MBS methodology in view of the stochastic discharge harmonics makes the LO2 liquefaction grade. The answer is NO. The reason is that LO2 production is the **product** of the recursion rate and liquefacted boundary layer. For example at 16.13Hz (the liquefaction threshold) the LO2 production rate is 0.01x3x16.13 = 0.48inch/sec. Conversely at at 100Hz (viz. 0.01sec) the LO2 production rate = 0.01x100 = 1.0inch/sec. At 60Hz (viz. 0.0166sec) the LO2 production rate = 1x0.01x60 = 0.6inch/sec, at 40Hz (viz. 0.025sec) the LO2 production rate = 1x0.01x40 = 0.4inch/sec, at 30Hz (viz. 0.033sec) the LO2 production rate = 2x0.01x30 = 0.6inch/sec which renders a numerical average of **0.5inch/sec** (which is perfectly predictable within the scope of a Gaussian distribution).

Ultimately the rate of LO2 production will be a function of the parametric fit, cost/performance optimization, the cryogenic (propellant) resource and the nature of the payload and/OR aerospace plane mission. Ditto presolved optimal DP strategies with a companion Kalman optimal gain filter.

4. FORTRAN and VISUAL BASIC Adaptations

Whereas the MBS liquefaction loop has been manually managed to date, the liquefaction loop may be automated via a Visual Basic OR programmed in Fortran with a graphics kit. Because the Fourier transient heat conduction DE conforms as the foundation of the MBS methodology, the MBS constitutes a powerful parametric design tool and real time stochastic estimation and optimal control recursion because of the perfectly linear computational structure.

5. Conclusion and Occolades

Hypersonic liquefaction and shockwave management and suppression has been an elusive misnomer to the scientific community throughout the space-age era because of explosive shockwave propagation that masked the underlying simplicity of cryogenic liquefaction and isothermal compression. The harmonic nature of the liquefaction process and the conformity of rules thereto however came as a surprise. The Crysonix project nonetheless has been the product of extreme perseverance and fortunate timing. All the kudu's however to the VT Aerospace and Ocean Laboratory directorate for making the facilitation and expertise available. Ditto the old fashioned wisdom of Messrs Binder and Schmidt. The crux of liquefaction however is the art of transient heat transfer and crossing all the T's.

ACKNOWLEDGEMENTS

Virginia State University, Blacksburg VA, Dept of Aerospace and Ocean Engineering Engineering

ANNEXURES

PART 1: Incremental time function

ΔL = 0.01

k2 = 0.44   ρ = 1.0   Cp = 0.22

α = k/ρCp = 0.44/(1.0x0.22) = 2.0

ΔΓ = dL^2 / 2 x α

ΔΓ = 3600x(0.01/12)^2 / 2x2.0 = 0.00062sec

PART 2: Differencing module boundary conditions

T(m, n+1) =T(m-1, n+1) -(dX/(dX/2+z2))*(T(m-1, n+1) -TK)

T(m, n+1) =T(m-1, n+1) -(dX/(dX/2+z2))*(T(m-1, n+1) -TF)

TW(n+1) =(T(m, n+1) +T(m+1, n+1))/2

T(m, n+1) =T(m-1, n) +T(m+1, n))/2

T(m, n+1) =T(m-1, n) +TK)/2

Zf =Ql/Cp = 90 / 0.44 = 209F

PART 3: The heat of transformations source terms

QL	92	92	92	92	92	92	92	92	92	92	92	92	92	92
kO2	0.44	0.44	0.44	0.44	0.44	0.44	0.44	0.44	0.44	0.44	0.44	0.44	0.44	0.44
ZF(F)	209	209	209	209	209	209	209	209	209	209	209	209	209	209
Tf (R)	220	220	220	220	220	220	220	220	220	220	220	220	220	220

PART 4: The structured computational model

	-140C	k	h	k/h	-160	-105C										Degerees Renkine					0.01	ΔL
	240	0.44	100	0.20	200	0	1	2	3	4	5	6	7	8	9	10	11	12	0		**0.000620**	ΔΓ
0	240	0.44	100	0.004	200	300	300	300	300	300	300	300	300	300	300	300	300	300	300		0.000000	n/a
1	240	0.44	100	0.004	200	200	250	275	288	294	297	298	299	300	300	300	300	300	300		0.000620	**1.34**
2	240	0.44	100	0.004	200	200	**238**	263	278	288	293	296	298	299	299	300	300	300	300	0	0.001240	0.67
3	240	0.44	100	0.004	200	200	**240**	259	273	283	290	294	296	298	299	299	300	300	300	9	0.001860	0.45
4	240	0.44	100	0.004	200	200	**240**	257	270	280	287	292	295	297	298	299	299	300	300	10	0.002480	0.34
5	240	0.44	100	0.004	200	200	**240**	255	267	277	284	289	293	296	297	298	299	299	300	12	0.003100	0.27
6	240	0.44	100	0.004	200	200	**240**	254	265	275	282	288	292	294	296	298	299	299	300	13	0.003720	0.22
7	240	0.44	100	0.004	200	200	**240**	253	264	273	280	286	290	293	295	297	298	299	300	13	0.004340	0.19

PART 5: The terminal saturation stage

94	240	0.44	100	0.004	200	200	220	240	**240**	246	252	258	264	270	276	282	288	294	300	7	0.058280	0.04
95	240	0.44	100	0.004	200	200	220	240	**240**	246	252	258	264	270	276	282	288	294	300	7	0.058900	0.04
96	240	0.44	100	0.004	200	200	220	240	**240**	246	252	258	264	270	276	282	288	294	300	7	0.059520	0.04
97	240	0.44	100	0.004	200	200	220	240	**240**	246	252	258	264	270	276	282	288	294	300	7	0.060140	0.04
98	240	0.44	100	0.004	200	200	220	240	**240**	246	252	258	264	270	276	282	288	294	300	7	0.060760	0.04
99	240	0.44	100	0.004	200	200	220	240	**240**	246	252	258	264	270	276	282	288	294	300	7	0.061380	0.04
100	240	0.44	100	0.004	200	200	220	240	**240**	246	252	258	264	270	276	282	288	294	300	7	**0.062000**	0.04
101	240	0.44	100	0.004	200	200	220	240	243	248	253	258	264	270	276	282	288	294	300	219	0.062620	**16.13**
102	240	0.44	100	0.004	200	200	220	240	244	248	253	259	264	270	276	282	288	294	300		0.063240	**Herz**
103	240	0.44	100	0.004	200	200	220	240	244	249	254	259	265	270	276	282	288	294	300		0.063860	

PART 6: The spreadsheet model

APPENDED

FIGURES

Figure1: Apparatus and testing cube configurations

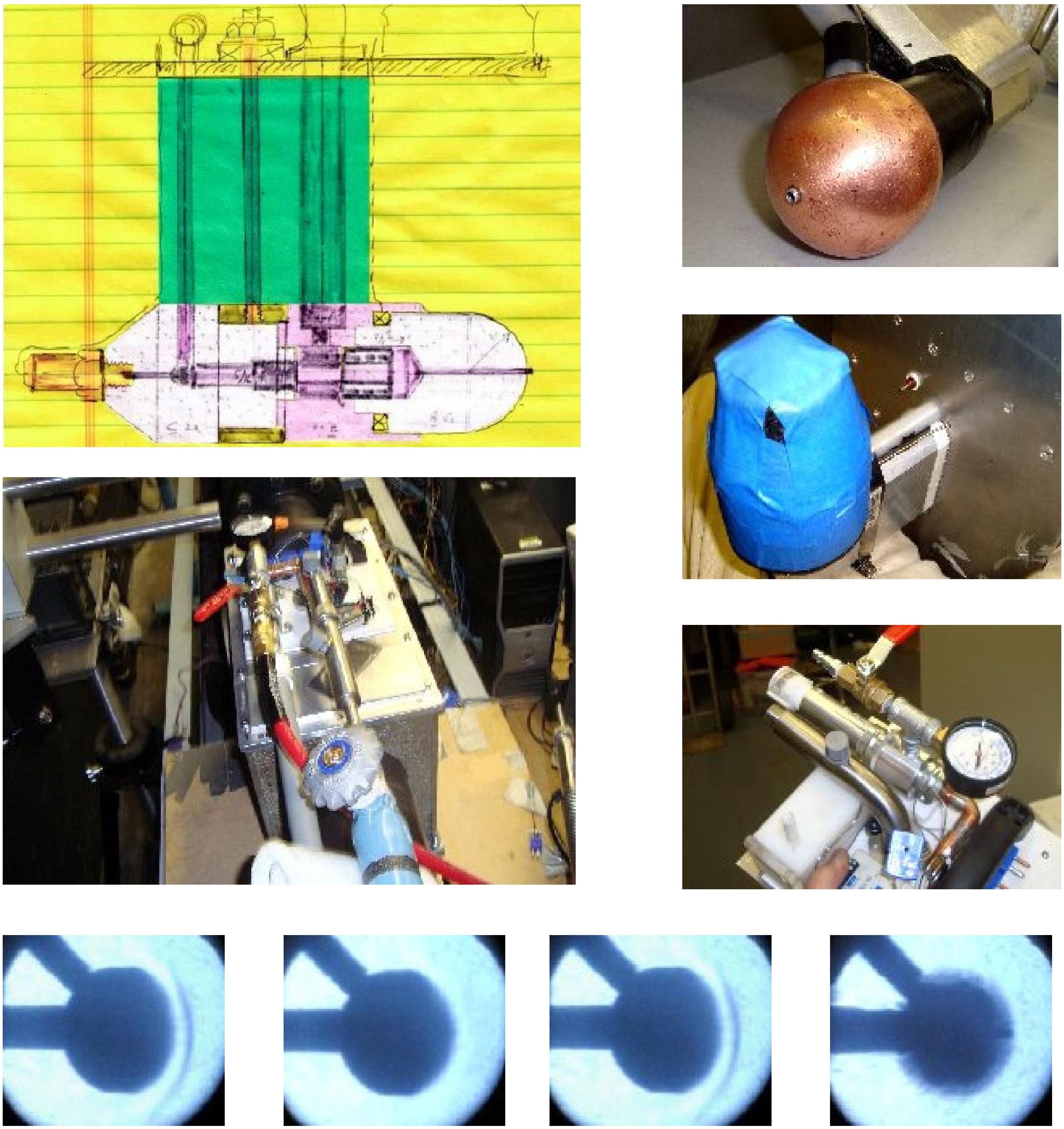

Figure 2: Dec 2010 harmonics

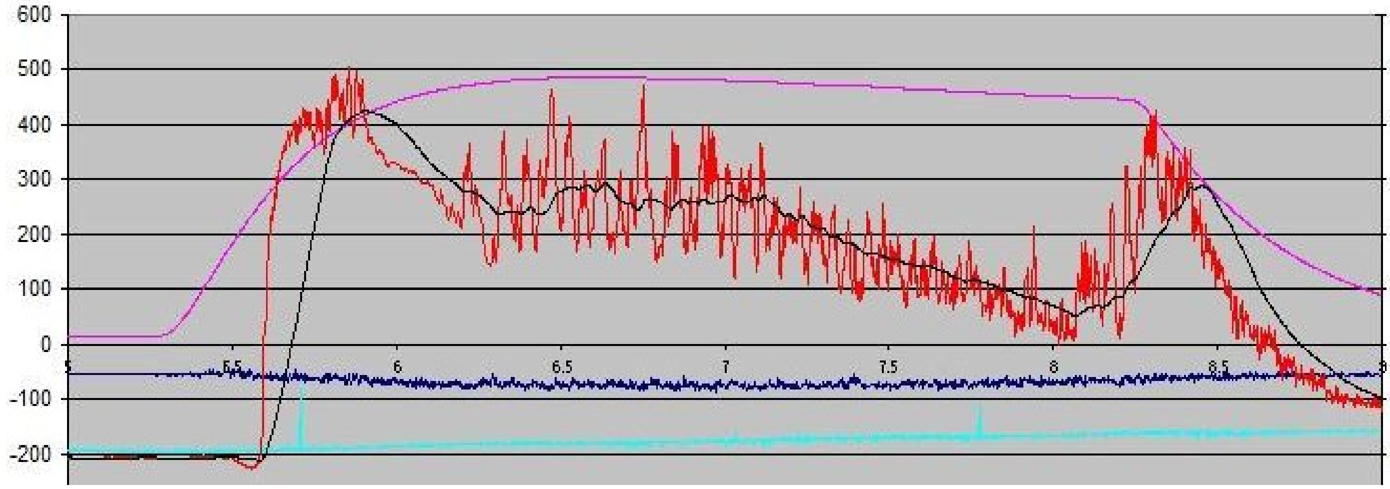

Figure 3: May 2011 harmonics

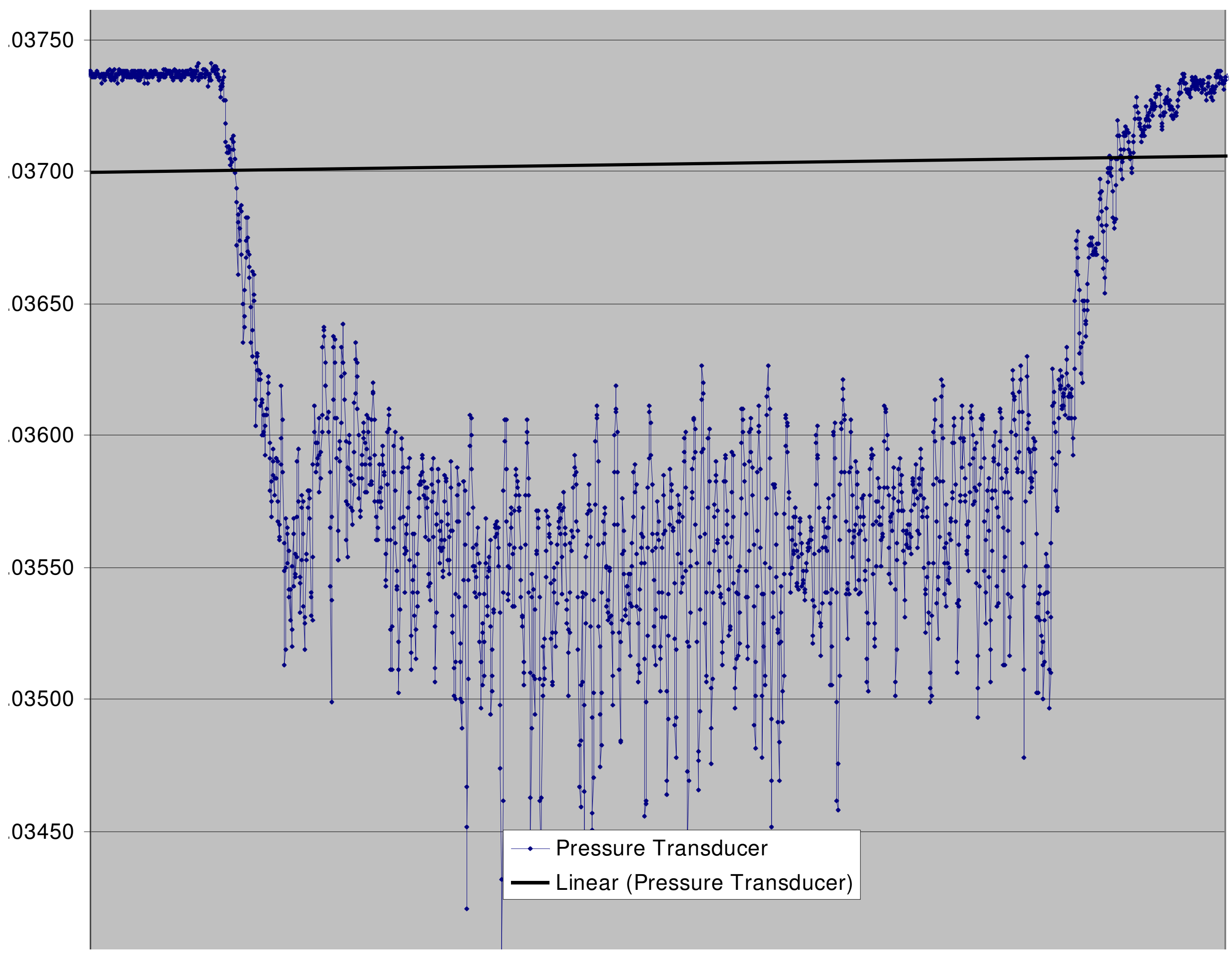

SPINNX© M5 BINDER-SCHMIDT LIQUEFACTION MODEL **Copyright Kartago Inc; Charl E Janeke (PE)** **7/9/13**

T(m, n+1) =T(m-1, n+1) -(dX/(dX/2+z2))*(T(m-1, n+1) -TK)
T(m, n+1) =T(m-1, n+1) -(dX/(dX/2+z2))*(T(m-1, n+1) -TF)
TW(n+1) =(T(m, n+1) +T(m+1, n+1))/2
T(m, n+1) =T(m-1, n) +T(m+1, n))/2
T(m, n+1) =T(m-1, n) +TK)/2
Zf =Ql/Cp = 90 / 0.44 = 209F

ΔL = 0.01
k2 = 0.44 ρ = 1.0 Cp = 0.22
α = k/ρCp = 0.44/(1.0x0.22) = 2.0
ΔΓ = dL^2 / 2 x α
ΔΓ = 3600x(0.01/12)^2 / 2x2.0 = 0.00062sec
12x LAYERS

QL	92	92	92	92	92	92	92	92	92	92	92	92	92	92	
kO2	0.44	0.44	0.44	0.44	0.44	0.44	0.44	0.44	0.44	0.44	0.44	0.44	0.44	0.44	
ZF(F)	209	209	209	209	209	209	209	209	209	209	209	209	209	209	QL/ k
Tf (R)	220	220	220	220	220	220	220	220	220	220	220	220	220	220	Tlatent

	-140C	k	h	k/h	-160	-105C								Degerees Renkine							0.01	ΔL
	240	0.44	100	0.20	200	0	1	2	3	4	5	6	7	8	9	10	11	12	0			0.000620	ΔΓ
0	240	0.44	100	0.004	200	300	300	300	300	300	300	300	300	300	300	300	300	300	300			0.000000	n/a
1	240	0.44	100	0.004	200	200	250	275	288	294	297	298	299	300	300	300	300	300	300			0.000620	**1.34**
2	240	0.44	100	0.004	200	200	**238**	263	278	288	293	296	298	299	299	300	300	300	300	0		0.001240	0.67
3	240	0.44	100	0.004	200	200	**240**	259	273	283	290	294	296	298	299	299	300	300	300	9		0.001860	0.45
4	240	0.44	100	0.004	200	200	**240**	257	270	280	287	292	295	297	298	299	299	300	300	10		0.002480	0.34
5	240	0.44	100	0.004	200	200	**240**	255	267	277	284	289	293	296	297	298	299	299	300	12		0.003100	0.27
6	240	0.44	100	0.004	200	200	**240**	254	265	275	282	288	292	294	296	298	299	299	300	13		0.003720	0.22
7	240	0.44	100	0.004	200	200	**240**	253	264	273	280	286	290	293	295	297	298	299	300	13		0.004340	0.19
8	240	0.44	100	0.004	200	200	**240**	252	262	271	279	284	289	292	295	296	298	299	300	14		0.004960	0.17
9	240	0.44	100	0.004	200	200	**240**	251	261	270	277	283	288	291	294	296	297	299	300	14		0.005580	0.15
10	240	0.44	100	0.004	200	200	**240**	251	260	269	276	282	286	290	293	295	297	298	300	14		0.006200	0.13
11	240	0.44	100	0.004	200	200	**240**	250	259	268	275	281	285	289	292	294	296	298	300	15		0.006820	0.12
12	240	0.44	100	0.004	200	200	**240**	250	259	267	274	279	284	288	291	294	296	298	300	15		0.007440	0.11
13	240	0.44	100	0.004	200	200	**240**	249	258	266	273	278	283	287	291	293	296	298	300	15		0.008060	0.10
14	240	0.44	100	0.004	200	200	**240**	249	257	265	272	278	282	287	290	293	295	298	300	15		0.008680	0.10
15	240	0.44	100	0.004	200	200	**240**	249	257	264	271	277	282	286	289	292	295	297	300	15		0.009300	0.09
16	240	0.44	100	0.004	200	200	**240**	248	256	264	270	276	281	285	289	292	295	297	300	16		0.009920	0.08
17	240	0.44	100	0.004	200	200	**240**	248	256	263	269	275	280	284	288	291	294	297	300	16		0.010540	0.08
18	240	0.44	100	0.004	200	200	**240**	248	255	262	269	274	279	284	288	291	294	297	300	16		0.011160	0.07
19	240	0.44	100	0.004	200	200	224	**240**	251	260	267	273	279	283	287	291	294	297	300	222	0	0.011780	**0.14**
20	240	0.44	100	0.004	200	200	220	**240**	250	259	266	272	278	282	286	290	294	297	300		5	0.012400	0.13
21	240	0.44	100	0.004	200	200	220	**240**	249	258	265	271	277	282	286	290	293	297	300		5	0.013020	0.13
22	240	0.44	100	0.004	200	200	220	**240**	249	257	264	270	276	281	285	289	293	296	300		5	0.013640	0.12
23	240	0.44	100	0.004	200	200	220	**240**	248	256	263	270	275	280	285	289	293	296	300		6	0.014260	0.12
24	240	0.44	100	0.004	200	200	220	**240**	248	256	263	269	275	280	284	288	292	296	300		6	0.014880	0.11
25	240	0.44	100	0.004	200	200	220	**240**	248	255	262	268	274	279	284	288	292	296	300		6	0.015500	0.11
26	240	0.44	100	0.004	200	200	220	**240**	248	255	262	268	274	279	283	288	292	296	300		6	0.016120	0.10
27	240	0.44	100	0.004	200	200	220	**240**	247	255	261	267	273	278	283	287	292	296	300		6	0.016740	0.10
28	240	0.44	100	0.004	200	200	220	**240**	247	254	261	267	273	278	283	287	292	296	300		6	0.017360	0.10
29	240	0.44	100	0.004	200	200	220	**240**	247	254	260	267	272	277	282	287	291	296	300		6	0.017980	0.09

30	240	0.44	100	0.004	200	200	220	**240**	247	254	260	266	272	277	282	287	291	296	300		6	0.018600	0.09
31	240	0.44	100	0.004	200	200	220	**240**	247	253	260	266	271	277	282	286	291	295	300		7	0.019220	0.09
32	240	0.44	100	0.004	200	200	220	**240**	247	253	260	265	271	276	281	286	291	295	300		7	0.019840	0.08
33	240	0.44	100	0.004	200	200	220	**240**	247	253	259	265	271	276	281	286	291	295	300		7	0.020460	0.08
34	240	0.44	100	0.004	200	200	220	**240**	247	253	259	265	270	276	281	286	291	295	300		7	0.021080	0.08
35	240	0.44	100	0.004	200	200	220	**240**	246	253	259	265	270	276	281	286	290	295	300		7	0.021700	0.08
36	240	0.44	100	0.004	200	200	220	**240**	246	253	259	264	270	275	280	285	290	295	300		7	0.022320	0.07
37	240	0.44	100	0.004	200	200	220	**240**	246	252	258	264	270	275	280	285	290	295	300		7	0.022940	0.07
38	240	0.44	100	0.004	200	200	220	**240**	246	252	258	264	270	275	280	285	290	295	300		7	0.023560	0.07
39	240	0.44	100	0.004	200	200	220	**240**	246	252	258	264	269	275	280	285	290	295	300		7	0.024180	0.07
40	240	0.44	100	0.004	200	200	220	**240**	246	252	258	264	269	275	280	285	290	295	300		7	0.024800	0.07
41	240	0.44	100	0.004	200	200	220	**240**	246	252	258	264	269	274	280	285	290	295	300		7	0.025420	0.07
42	240	0.44	100	0.004	200	200	220	**240**	246	252	258	263	269	274	280	285	290	295	300		7	0.026040	0.06
43	240	0.44	100	0.004	200	200	220	**240**	246	252	258	263	269	274	279	285	290	295	300		7	0.026660	0.06
44	240	0.44	100	0.004	200	200	220	**240**	246	252	258	263	269	274	279	285	290	295	300		7	0.027280	0.06
45	240	0.44	100	0.004	200	200	220	**240**	246	252	257	263	269	274	279	285	290	295	300		7	0.027900	0.06
46	240	0.44	100	0.004	200	200	220	**240**	246	252	257	263	268	274	279	284	290	295	300		7	0.028520	0.06
47	240	0.44	100	0.004	200	200	220	**240**	246	252	257	263	268	274	279	284	290	295	300		7	0.029140	0.06
48	240	0.44	100	0.004	200	200	220	**240**	246	252	257	263	268	274	279	284	290	295	300		7	0.029760	0.06
49	240	0.44	100	0.004	200	200	220	**240**	246	251	257	263	268	274	279	284	290	295	300		7	0.030380	0.05
50	240	0.44	100	0.004	200	200	220	**240**	246	251	257	263	268	274	279	284	289	295	300		7	0.031000	0.05
51	240	0.44	100	0.004	200	200	220	**240**	246	251	257	263	268	273	279	284	289	295	300		7	0.031620	0.05
52	240	0.44	100	0.004	200	200	220	**240**	246	251	257	263	268	273	279	284	289	295	300		7	0.032240	0.05
53	240	0.44	100	0.004	200	200	220	233	242	250	256	262	268	273	279	284	289	295	300		217	0.032860	**0.08**
54	240	0.44	100	0.004	200	200	216	229	**239**	248	255	261	267	273	279	284	289	295	300	0		0.033480	0.07
55	240	0.44	100	0.004	200	200	215	227	**240**	247	254	261	267	273	278	284	289	295	300	3		0.034100	0.07
56	240	0.44	100	0.004	200	200	214	227	**240**	247	254	260	267	272	278	284	289	295	300	3		0.034720	0.07
57	240	0.44	100	0.004	200	200	213	227	**240**	247	254	260	266	272	278	284	289	295	300	3		0.035340	0.07
58	240	0.44	100	0.004	200	200	213	227	**240**	247	254	260	266	272	278	283	289	294	300	3		0.035960	0.07
59	240	0.44	100	0.004	200	200	213	227	**240**	247	253	260	266	272	278	283	289	294	300	3		0.036580	0.07
60	240	0.44	100	0.004	200	200	213	227	**240**	247	253	260	266	272	277	283	289	294	300	3		0.037200	0.07
61	240	0.44	100	0.004	200	200	213	227	**240**	247	253	259	266	271	277	283	289	294	300	3		0.037820	0.07
62	240	0.44	100	0.004	200	200	213	227	**240**	247	253	259	265	271	277	283	289	294	300	3		0.038440	0.07
63	240	0.44	100	0.004	200	200	213	227	**240**	246	253	259	265	271	277	283	289	294	300	3		0.039060	0.06
64	240	0.44	100	0.004	200	200	213	227	**240**	246	253	259	265	271	277	283	289	294	300	3		0.039680	0.06
65	240	0.44	100	0.004	200	200	213	227	**240**	246	253	259	265	271	277	283	289	294	300	3		0.040300	0.06
66	240	0.44	100	0.004	200	200	213	227	**240**	246	253	259	265	271	277	283	288	294	300	3		0.040920	0.06
67	240	0.44	100	0.004	200	200	213	227	**240**	246	253	259	265	271	277	283	288	294	300	3		0.041540	0.06
68	240	0.44	100	0.004	200	200	213	227	**240**	246	253	259	265	271	277	283	288	294	300	4		0.042160	0.06
69	240	0.44	100	0.004	200	200	213	227	**240**	246	252	259	265	271	277	282	288	294	300	4		0.042780	0.06
70	240	0.44	100	0.004	200	200	213	227	**240**	246	252	259	265	271	277	282	288	294	300	4		0.043400	0.06
71	240	0.44	100	0.004	200	200	213	227	**240**	246	252	258	265	271	276	282	288	294	300	4		0.044020	0.06
72	240	0.44	100	0.004	200	200	213	227	**240**	246	252	258	264	270	276	282	288	294	300	4		0.044640	0.06
73	240	0.44	100	0.004	200	200	213	227	**240**	246	252	258	264	270	276	282	288	294	300	4		0.045260	0.06
74	240	0.44	100	0.004	200	200	213	227	**240**	246	252	258	264	270	276	282	288	294	300	4		0.045880	0.05
75	240	0.44	100	0.004	200	200	213	227	**240**	246	252	258	264	270	276	282	288	294	300	4		0.046500	0.05

76	240	0.44	100	0.004	200	200	213	227	**240**	246	252	258	264	270	276	282	288	294	300	4	0.047120	0.05
77	240	0.44	100	0.004	200	200	213	227	**240**	246	252	258	264	270	276	282	288	294	300	4	0.047740	0.05
78	240	0.44	100	0.004	200	200	213	227	**240**	246	252	258	264	270	276	282	288	294	300	4	0.048360	0.05
79	240	0.44	100	0.004	200	200	213	227	**240**	246	252	258	264	270	276	282	288	294	300	4	0.048980	0.05
80	240	0.44	100	0.004	200	200	213	227	**240**	246	252	258	264	270	276	282	288	294	300	4	0.049600	0.05
81	240	0.44	100	0.004	200	200	213	227	**240**	246	252	258	264	270	276	282	288	294	300	4	0.050220	0.05
82	240	0.44	100	0.004	200	200	213	227	**240**	246	252	258	264	270	276	282	288	294	300	4	0.050840	0.05
83	240	0.44	100	0.004	200	200	213	227	**240**	246	252	258	264	270	276	282	288	294	300	4	0.051460	0.05
84	240	0.44	100	0.004	200	200	213	227	**240**	246	252	258	264	270	276	282	288	294	300	4	0.052080	0.05
85	240	0.44	100	0.004	200	200	213	240	**240**	246	252	258	264	270	276	282	288	294	300	7	0.052700	0.05
86	240	0.44	100	0.004	200	200	220	240	**240**	246	252	258	264	270	276	282	288	294	300	7	0.053320	0.05
87	240	0.44	100	0.004	200	200	220	240	**240**	246	252	258	264	270	276	282	288	294	300	7	0.053940	0.05
88	240	0.44	100	0.004	200	200	220	240	**240**	246	252	258	264	270	276	282	288	294	300	7	0.054560	0.05
89	240	0.44	100	0.004	200	200	220	240	**240**	246	252	258	264	270	276	282	288	294	300	7	0.055180	0.05
90	240	0.44	100	0.004	200	200	220	240	**240**	246	252	258	264	270	276	282	288	294	300	7	0.055800	0.04
91	240	0.44	100	0.004	200	200	220	240	**240**	246	252	258	264	270	276	282	288	294	300	7	0.056420	0.04
92	240	0.44	100	0.004	200	200	220	240	**240**	246	252	258	264	270	276	282	288	294	300	7	0.057040	0.04
93	240	0.44	100	0.004	200	200	220	240	**240**	246	252	258	264	270	276	282	288	294	300	7	0.057660	0.04
94	240	0.44	100	0.004	200	200	220	240	**240**	246	252	258	264	270	276	282	288	294	300	7	0.058280	0.04
95	240	0.44	100	0.004	200	200	220	240	**240**	246	252	258	264	270	276	282	288	294	300	7	0.058900	0.04
96	240	0.44	100	0.004	200	200	220	240	**240**	246	252	258	264	270	276	282	288	294	300	7	0.059520	0.04
97	240	0.44	100	0.004	200	200	220	240	**240**	246	252	258	264	270	276	282	288	294	300	7	0.060140	0.04
98	240	0.44	100	0.004	200	200	220	240	**240**	246	252	258	264	270	276	282	288	294	300	7	0.060760	0.04
99	240	0.44	100	0.004	200	200	220	240	**240**	246	252	258	264	270	276	282	288	294	300	7	0.061380	0.04
100	240	0.44	100	0.004	200	200	220	240	**240**	246	252	258	264	270	276	282	288	294	300	7	**0.062000**	0.04
101	240	0.44	100	0.004	200	200	220	240	243	248	253	258	264	270	276	282	288	294	300	219	0.062620	**16.13**
102	240	0.44	100	0.004	200	200	220	240	244	248	253	259	264	270	276	282	288	294	300		0.063240	**Herz**
103	240	0.44	100	0.004	200	200	220	240	244	249	254	259	265	270	276	282	288	294	300		0.063860	
104	240	0.44	100	0.004	200	200	220	240	244	249	254	259	265	271	276	282	288	294	300		0.064480	
105	240	0.44	100	0.004	200	200	220	240	245	249	254	260	265	271	276	282	288	294	300		0.065100	
106	240	0.44	100	0.004	200	200	220	240	245	249	255	260	265	271	277	282	288	294	300		0.065720	
107	240	0.44	100	0.004	200	200	220	240	245	250	255	260	265	271	277	282	288	294	300		0.066340	
108	240	0.44	100	0.004	200	200	220	240	245	250	255	260	266	271	277	283	288	294	300		0.066960	
109	240	0.44	100	0.004	200	200	220	240	245	250	255	260	266	271	277	283	288	294	300		0.067580	
110	240	0.44	100	0.004	200	200	220	240	245	250	255	260	266	271	277	283	288	294	300		0.068200	
111	240	0.44	100	0.004	200	200	220	240	245	250	255	261	266	271	277	283	289	294	300		0.068820	
112	240	0.44	100	0.004	200	200	220	240	245	250	255	261	266	272	277	283	289	294	300		0.069440	
113	240	0.44	100	0.004	200	200	220	240	245	250	255	261	266	272	277	283	289	294	300		0.070060	
114	240	0.44	100	0.004	200	200	220	240	245	250	256	261	266	272	277	283	289	294	300		0.070680	
115	240	0.44	100	0.004	200	200	220	240	245	250	256	261	266	272	277	283	289	294	300		0.071300	
116	240	0.44	100	0.004	200	200	220	240	245	250	256	261	266	272	277	283	289	294	300		0.071920	
117	240	0.44	100	0.004	200	200	220	240	245	250	256	261	266	272	278	283	289	294	300		0.072540	
118	240	0.44	100	0.004	200	200	220	240	245	250	256	261	267	272	278	283	289	294	300		0.073160	
119	240	0.44	100	0.004	200	200	220	240	245	250	256	261	267	272	278	283	289	294	300		0.073780	
120	240	0.44	100	0.004	200	200	220	240	245	251	256	261	267	272	278	283	289	294	300		0.074400	
121	240	0.44	100	0.004	200	200	220	240	245	251	256	261	267	272	278	283	289	294	300		0.075020	

Binder-Schmidt Cryogenic Liquefaction Model; Copyright: Charl E Janeke PE / Kartago Inc / July 2013 (Mach-5 Dynamics)